INTERNATIONAL SOCIETY FOR
SOIL MECHANICS AND
GEOTECHNICAL ENGINEERING

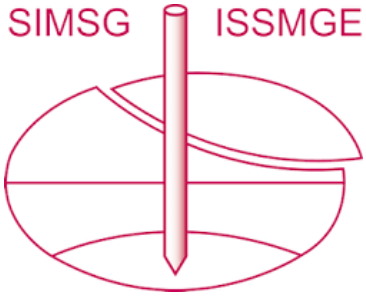

This paper was downloaded from the Online Library of the International Society for Soil Mechanics and Geotechnical Engineering (ISSMGE). The library is available here:

https://www.issmge.org/publications/online-library

This is an open-access database that archives thousands of papers published under the Auspices of the ISSMGE and maintained by the Innovation and Development Committee of ISSMGE.

Three Questions on the Stability of Slopes

Trois Questions de la stabilité des talus

V. MENCL, DR.SC., *Professor, Technical University, Brno, Czechoslovakia*
P. PETER, *Professor, Technical University, Bratislava, Czechoslovakia*
J. JESENÁK, C.SC., *Technical University, Bratislava, Czechoslovakia*
J. ŠKOPEK, ING.C.SC., *Scientific Worker, Institute of Geological Investigations, Praha, Czechoslovakia*

SUMMARY

Part I deals with the influence of residual stress in clayey deposits on the slope stability of excavations. The author describes an attempt to measure these stresses in the field and refers to a case where the method was successful.

Part II describes investigations on the stability of the thin topsoil layer on the slopes of embankments with four different phases, dependent on the angle of slope, the shear strength of topsoil, and the duration of rainfall.

Part III deals with the determination of the shearing strength of fissured clays with significant horizontal joints. The strength has been tested in a triaxial compression test on samples taken vertically or obliquely and in field shearing tests. The results of the tests in the field and in the laboratory are close to each other.

SOMMAIRE

La première partie traite de l'influence des tensions résiduelles dans les couches argileuses sur la stabilité des talus des excavations. L'auteur décrit un essai de mesure de ces tensions en place et mentionne un autre cas où cette méthode a été appliquée avec succès.

La deuxième partie décrit des recherches sur la stabilité de la couche d'humus qui recouvre un talus sous quatre phases différentes, qui dépendent de l'angle du talus, de la résistance au cisaillement de la couche de sol et de la durée de la pluie.

La troisième partie traite de la determination de la résistance au cisaillement des argiles fissurées ayant des joints fortement horizontaux. La résistance au cisaillement a été determinée par des essais triaxiaux sur des échantillons prélevés verticalement ou obliquement et par des essais de cisaillement de chantier. Les résultats obtenus en laboratoire et sur le chantier sont du même ordre.

I. MEASUREMENT OF STRESSES IN SOIL MASSES

THE EXISTENCE OF RESIDUAL HORIZONTAL STRESSES in clayey deposits and their danger to the stability of slopes of excavations has been shown (Skempton, 1961). Further phenomena threatening the stability of such a slope include the following.

1. A slight movement in the direction towards the excavation results in diminishing the circumference of the cut, and therefore shear surfaces originate on the surface of the slopes. Fig. 1 shows such a shear surface visible in the wall of a drainage cut dug in the slope. Fig. 2 shows the outcrop

FIG. 1. Shear surface visible at the wall of a drainage cut.

FIG. 2. Outcrop of a shear on the surface of the slope.

of such a shear surface on the surface of the slope. At a depth of 5 to 6 m beneath the slope surface the shear surfaces disappear. These surfaces become opened by desiccation, water enters, and it is only a question of time whether or not failure will occur before the retaining walls can be erected.

2. The upper beds of the ground are very often younger than the lower beds in which the residual stresses are hidden. By horizontal movement of the lower beds the upper beds are either softened or torn into blocks. By studying the density of about 150 samples the authors have found that the density

FIG. 3. Sliding of the upper layers.

of clayey loam in the vicinity of the excavation was 93 per cent of that at a greater distance from the slope. This is why the first landslide occurred in the surface beds of the excavation (Fig. 3).

3. By residual horizontal forces the bottom of the excavation is heaved up and, as a rule, it is not until afterwards (several months after the slide in 2) that the slide of the whole slope begins (Fig. 4).

FIG. 4. Sliding of the entire slope.

It is a strange phenomenon that the features described exist at some sites whereas at others the slopes are stable without any retaining structure. An attempt was made, therefore, to measure the residual stresses by means of the "removal of material technique," initiated by Sachs (Dow, 1956). A cylindrical hole (Fig. 5) is bored in the ground and the displacements of points around the hole are measured by means of strain gauges. Lamé's constants of the soil being known, the stresses in the mass of soil can be computed by using the following formulae.

In the case of axial symmetry:

$$\sigma = (\Delta r \cdot r \cdot E)/(1 + \eta)a^2,$$

where Δr is the movement of observed point (σ is pressure if Δr is in the direction towards the centre), a is the radius of the hole.

FIG. 5. The arrangement of the hole and of the strain gauges.

In the case of different stresses in two directions, σ_1 and σ_2, the point lying in the line parallel to σ_1 moves Δr_1. Analogously, Δr_2 is the movement of the point lying in the centre arrow parallel to σ_2. Considering Δr as positive if the point moves toward the centre and considering σ as positive if it is compression, σ_1 and σ_2 can be computed from:

$$\Delta r_1 = \frac{\sigma_1}{2E}\frac{a^2}{r}\left[5 + \eta - \frac{a^2}{r^2}(1 - \eta)\right] + \frac{\sigma_2}{2E}\frac{a^2}{r}\left[-3 + \eta + \frac{a^2}{r^2}(1 + \eta)\right]$$

$$\Delta r_2 = \frac{\sigma_1}{2E}\frac{a^2}{r}\left[-3 + \eta + \frac{a^2}{r^2}(1 + \eta)\right] + \frac{\sigma_2}{2E}\frac{a^2}{r}\left[5 + \eta - \frac{a^2}{r^2}(1 - \eta)\right].$$

By repeating the measurement very often, at least a qualitative picture of the stresses can be made. But by substituting the probable values of Lamé's constants (for example $E = 170$ kp/sq.cm. and $\eta = 0.4$ for a Tertiary clay), the probable value of σ is obtained (for example on the site for a large hotel structure in Brno, the author obtained $\sigma = 1.1$ kp/sq.cm. at the depth of 2 m below the surface of the Neogene clay).

The method works well even in other conditions. Fig. 6 shows the cross-section of an old landslide in a Paleogene clay, in the basin of an earth dam under construction. Because of the very slow movement of the slide (of the order of 0.5 in. per year), analysis was difficult. But the measurement of stress indicated tensile stress at point a, compression at point b, and zero stress at point c. It could be concluded that the slide occupies only the area a to c and that at point c a more stable bedrock is to be expected. Indeed, the borings at c proved the existence of an hidden Pleistocene rock terrace.

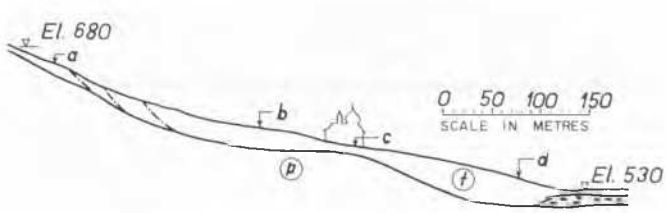

FIG. 6. Cross-section of a landslide at L. Mara: p, clayey shales of Paleogene; t, talus material.

II. STABILITY OF TOPSOIL LAYER ON THE SLOPES OF EMBANKMENTS

Hitherto the prerequisites concerning the flow of water at the interface of two soils of different permeabilities, e.g. the surface layer (silty soil) on the slopes of embankments and earth dams and gravel under them, were based largely on the simplified assumption that rainfall water penetrates the semi-permeable soil almost perpendicularly and later passes through the gravel almost vertically. In fact, very different methods of flow, including imbibition, seepage under the gravity forces, potential flow, and thermocapillary flow, play certain parts in this motion of water. The Van der Waal forces and the air resistance, as well as the electro-osmotic forces, generally retard and complicate the flow of water to such an extent as to render the exact mathematical analysis of the slope stability impossible.

Our observations in the field and our laboratory tests show that the change of the slope stability which occurs during and after the saturation of soil is mostly influenced by the velocity of imbibition which at the given depth z under the surface of the layer may be expressed with the imbibition coefficient k_v and the effective capillary height of the soil h_k as it results from the equation:

$$v = k_v(z \cos \beta + h_k)/z$$
$$= k_v(\cos \beta + h_k/z). \quad (1)$$

As the thickness of the protective layers is generally small (usually $d = \frac{1}{3} \sim \frac{2}{3} h_k$), the above critical velocities occur at the interface of semi-permeable and permeable soils resulting in the washing out of fine particles from the topsoil and their deposition on the surface of the more permeable soil. Thus the permeability of loam increases while that of gravel decreases. The change in the conditions of flow takes place with considerable flow of water not only normal to, but also along the interface of either soil.

On the model (Fig. 7) consisting of a layer of gravel 18–20 cm in thickness and of a layer of silty loam 10 to 20 cm in thickness, we observed both the conditions of flow and the conditions of stability. We used a flume 275 cm in length and 60 cm wide with adjustable tilt β. The fine-grained soil under investigation (unit weight γ = 1.7–1.78 ton/cu.m.; porosity η = 36–32 per cent; angle of internal friction ϕ = 20–26°; cohesion c_u = 0.05–0.02 Mp/sq.m.; capillary height h_k = 35–45 cm; coefficient of imbibition $k_v = 8 \times 10^{-5}$–4×10^{-3} cm/sec; permeability coefficient $k = 2.3 \times 10^{-5}$ cm/sec), was exposed to intensive sprinkling for intervals ranging from minutes to hours in order to simulate rainfall. This model and the auxiliary ones facilitated the investigation of both the conditions of flow of water and the stability of the covering layer in four phases.

In phase I, dry slope, the stability of the slope is given by the equation:

$$\gamma d \cos \beta \tan \phi = \gamma d \sin \beta - c_u. \quad (2)$$

In phase II, during the infiltration of water (with n = porosity of the soil):

$$d(\gamma + n\gamma_w) \cos \beta \tan \phi = (\gamma - n\gamma_w)d \sin \beta - c_u. \quad (3)$$

After water has penetrated the protective layer and the uplift as well as the hydrodynamic pressure takes effect at the lower surface of the former (the thickness of the layer in our model amounted to about 0.2 d) the third (III) phase is reached with the equilibrium expressed with the equation:

$$(\gamma - 0.2)d \cos \beta \tan \phi$$
$$= (\gamma - 0.2)d \sin \beta + 0.2d\gamma_w \sin \beta - c_u. \quad (4)$$

Phase IV calls for the highest value of the angle of internal friction if equilibrium is to be maintained; the value of ϕ_b can be arrived at in the equation

$$\tan \phi_b^{IV} = (1 + \gamma_w/\gamma') \tan \beta - (c_u/\gamma' d \cos \beta). \quad (5)$$

However, the equilibrium found by this equation comes into force only after the blanket has become disconnected (owing to tensile forces) into patches with fissures spaced at the distance l_{kr} that complies with:

$$l_{kr} = \frac{c_u \cot \phi(1 - k_n)}{\gamma' \sin \beta + \gamma_w \sin \beta - \frac{c_u}{d} \gamma' \cos \beta \tan \phi} \quad (6)$$

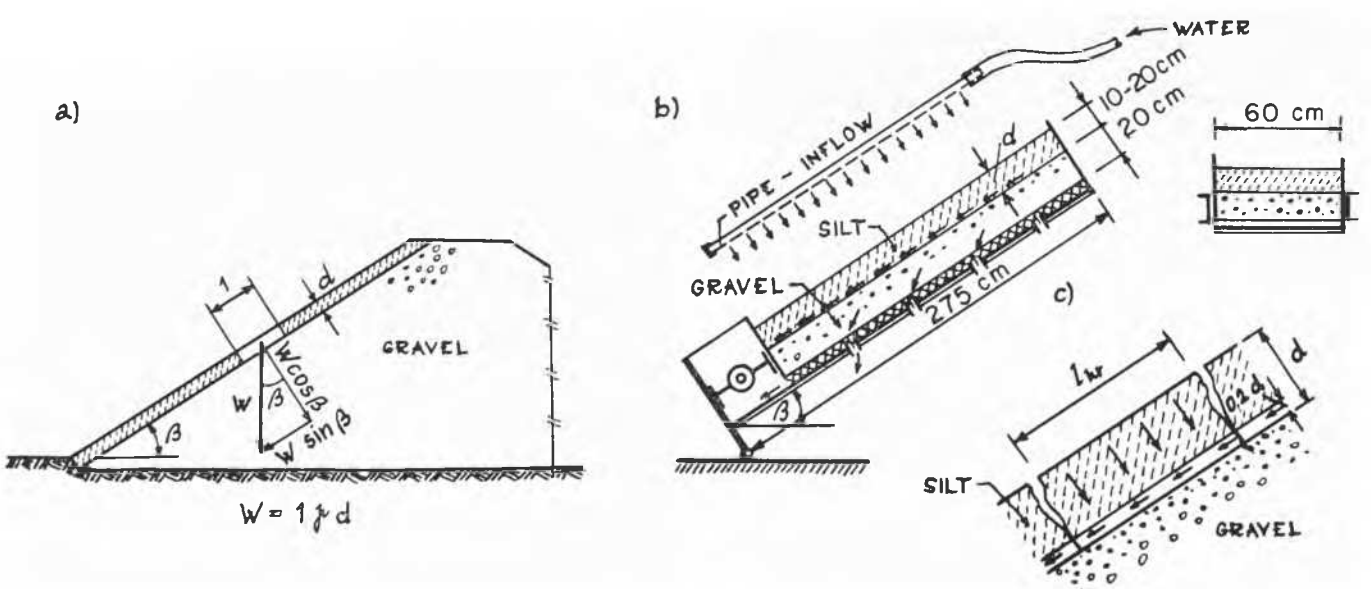

FIG. 7. Location of the layer and the model for the research on the flow of water and stability determination of silty soil. (a) Top soil on slope of embankment; (b) model; (c) Cracked layer.

where, apart from the symbols already mentioned, we introduce k_a, the coefficient of active earth pressure.

The requisite angle of internal friction for the individual phases I–IV, ϕ_b, can be determined on the basis of the presented and adjusted equations. For the frequent angle of slope $\beta = 30°$ and the thickness of protective silty layer $d = 0.1$–0.3 m, $c_u = 0.05$ Mp/sq.m., we obtain the following values of ϕ_b: Phase I, 10°20′–23°50′; Phase II, 13°45′–25°; Phase III, 16°30′–28°50′; Phase IV, 36°–44°50′. As soils with organic admixtures usually have an angle of internal friction $\phi = 18°$–$27°$, they provide, after saturation, unstable protective layers if the angle of slope $\beta = 30°$ and the apparent cohesion $c_u = 0.05$ Mp/sq.m. are used. The moment of failure is in the first place a function of the intensity and duration of rain and of the infiltration rate. The duration of infiltration can be approximately determined from the equation:

$$t_r = \int_0^d \frac{(w - w_0)z}{k_v(z \cos \beta + h_k)}\, dz \qquad (7)$$

where w_0, w is water content in per cent of volume before and after saturation, respectively.

From the standpoint of stability, after the expiration of this time, phase II and later (under the conditions stipulated before) phase III sets in, the latter being characterized by incipient uplift and flow of water at the interface of the protective layer and of the embankment, with the effect of hydrodynamic pressure according to Equation 4. Under the presumption of successive formation of fissures spaced l_{kr}, we obtain for this phase the critical time t_{kr} necessary for the change of stability to occur:

$$t_{kr} \cong t_v + n' l_{kr}/k \sin \beta,$$

with t_v = time of infiltration (see Eq 7), n' = effective porosity, k = permeability coefficient at the interface.

For the given values of $w = 0.38$; $w_0 = 0.18$; $\beta = 30°$; $h_k = 40$ cm; $k_v = 4 \times 10^{-3}$ to 8×10^{-5} cm/sec; $k = 10^{-3}$ cm/sec we obtain infiltration times of 0.45 ($d = 10$ cm), 0.86 ($d = 15$ cm), 2.62 ($d = 20$ cm), 8.34 ($d = 25$ cm), 26.40 ($d = 30$ cm), hours.

The most adverse state of equilibrium (IV) is expressed by the equation:

$$c_u/\gamma' d = (1 + \gamma_w/\gamma') \sin \beta - \tan \phi \cos \beta$$
$$\cong 2 \sin \beta - \tan \phi \cos \beta. \qquad (8)$$

Fig. 8 presents the values plotted by this equation as well as those plotted by the analogous equation for phase III.

III. TESTING THE SHEARING STRENGTH OF FISSURED CLAY

The Nechranice Dam is situated on the River Ohře. The embankment is 3280 m long and has a maximum height of 48 m. The underlying strata consist of flood plain gravel of an average thickness of 2–10 m. Beneath the gravel lies a thick bed of Miocene clay. In the geological period erosion caused the removal of at least 60 m of the upper part of this layer.

The clay is dark grey and is subdivided by fissures into fragments. Especially significant are the horizontal joints which extend continuously over a long distance. In the upper zone, where a considerable degree of softening accompanied the pressure release due to erosion of overlying beds, the clay is stiff. The lower clay is very stiff to hard. The clay has: $w_L = 56$–77 and $w_P = 26$–36; water content, 22–32 per cent; colloidal activity, 0.8; 55–65 per cent particles under 0.005 mm; $\phi' = 27°$–$33°$; and $c' = 0$–1.4 kp/sq.cm. There

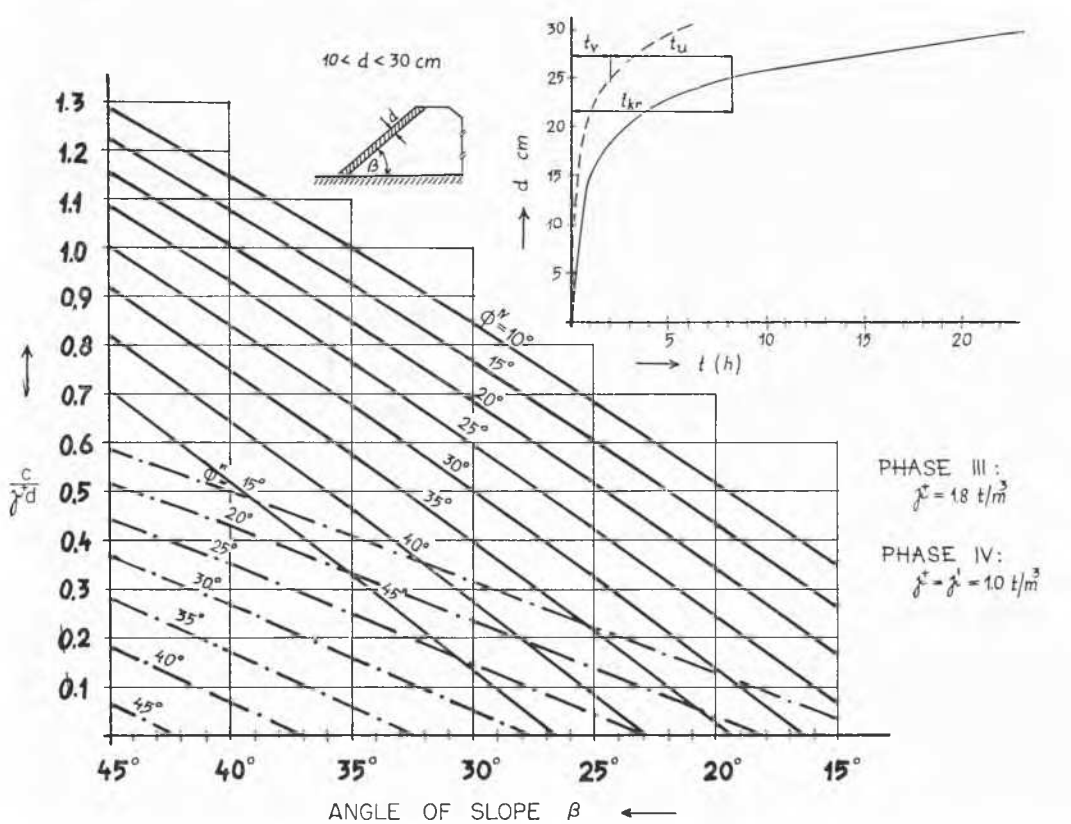

FIG. 8. Diagram indicating the conditions of stability for phases III and IV. ϕ^{III} applies to phase III, ϕ^{IV} applies to phase IV.

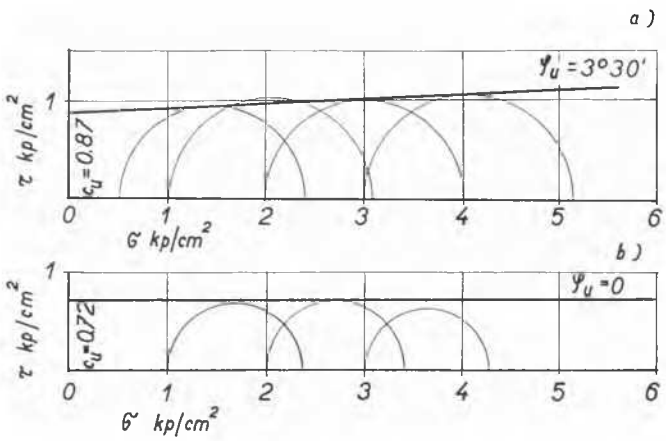

FIG. 9. Results of undrained triaxial tests: (a) samples taken vertically; (b) samples taken obliquely.

are considerable variations in strength both horizontally as well as vertically.

The shearing strength of fissured clay was tested firstly on undisturbed samples taken with a 100-mm-ID, thin-walled sampler. Undrained triaxial compression tests were carried out and the results of 186 tests are shown in Fig. 9a, where the average values are plotted.

The samples were cut vertically. The failure planes in the test were inclined and passed through relatively compact material. As there was the possibility of lower shear strength in the direction of horizontal joints, samples (100 mm diameter) were also taken with their axis inclined to the vertical so as to allow the failure planes to coincide with any horizontal planes of weakness. The result of 15 undrained triaxial tests is shown in Fig. 9b, where again average values are plotted.

Comparing the results of the two sets of samples, a drop in strength of about 27 per cent was found in the samples obliquely taken. This indicates that the shearing strength in the direction of horizontal joints may be expected to be lower than in any other direction. As the shearing strength in horizontal joints has a decisive influence on the stability of the dam, eleven field shearing tests were run.

The method used for field shearing tests was thoroughly described by Bukovanský (1962). The diagram of the test procedure is shown in Fig. 10. The tests were arranged so as to avoid, as much as possible, heave of the bottom of the test pit after excavation and to render possible the use of normal loads as high as 9 kp/sq.cm.

The steel shearing ring had a diameter of 70 cm and consisted of two parts. The upper part was 15 cm high; the lower part was 70 cm high and was provided with a cutting edge. Immediately after the excavation of the test pit, both shearing rings, one on top of the other, were placed on the bottom. A steel loading plate was inserted into the rings and loaded with a load equal to the overburden pressure, about 1.2 kp/sq.cm. (Fig. 10a). Both shearing rings were then pushed down into the clay (Fig. 10b). The clay around the upper ring was removed, the upper ring pushed up slightly to create a gap about 1 cm wide, and a horizontally acting jack was applied (Fig. 10c). The test was then started. Each test lasted about 1 to 2 hours. After the test the shearing rings were pushed down about 15 cm and the new test was prepared as before. The result of the tests is plotted in Fig. 10d. To determine how the horizontal joints affect the result of the test, the shearing test, using the normal load of 3 and 6 kp/sq.cm. was repeated in different, closely lying levels.

The result of the field tests confirmed that the strength of the clay is given by the strength in horizontal planes of weakness, which is much smaller than the strength outside these planes. Nevertheless, this strength under high normal stresses does not differ considerably from the strength determined by triaxial compression tests on vertically taken samples.

REFERENCES

BUKOVANSKÝ, M. (1962). Determination of the strength of claystones (in Czech). Docent thesis, Komenský University, Bratislava.

DOW, R. B. (1956). Some rheological properties under high pressure, Vol. 1. New York, Academic Press.

SKEMPTON, A. W. (1961). Horizontal stresses in an overconsolidated Eocene clay. *Proc. Fifth International Conference on Soil Mechanics and Foundation Engineering*, Vol. 1, pp. 351–7.

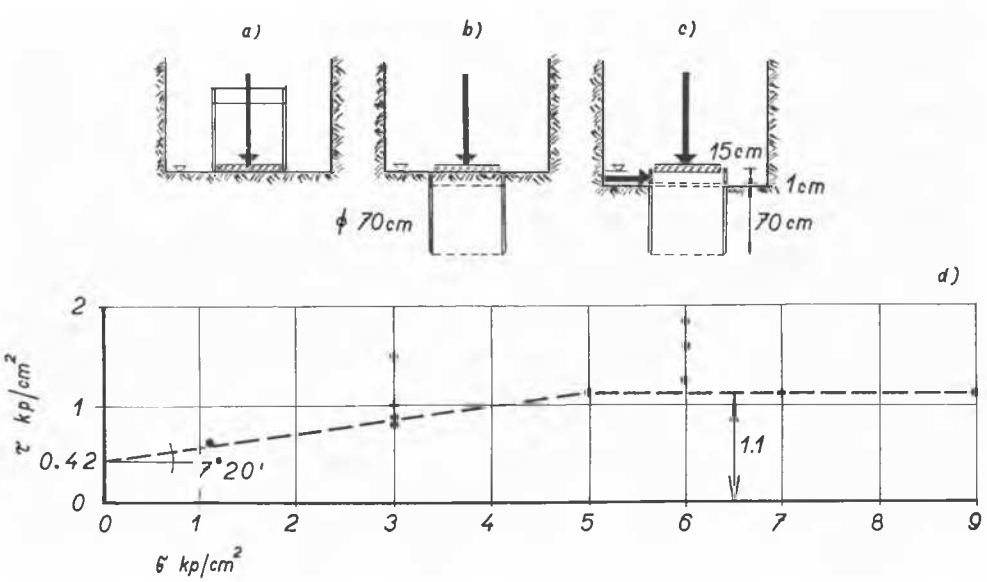

FIG. 10. Field shearing test: (a), (b), (c) diagram of test procedure; (d) values measured.